Biomaterials 156 (2018) 16–27

Contents lists available at ScienceDirect

Biomaterials

journal homepage: www.elsevier.com/locate/biomaterials

MSC exosomes mediate cartilage repair by enhancing proliferation, attenuating apoptosis and modulating immune reactivity

Shipin Zhang [a], Shang Jiunn Chuah [a], Ruenn Chai Lai [b], James Hoi Po Hui [c, d], Sai Kiang Lim [b, e], Wei Seong Toh [a, d, *]

[a] Faculty of Dentistry, National University of Singapore, Singapore
[b] Institute of Medical Biology, Agency for Science, Technology and Research, Singapore
[c] Cartilage Repair Program, Therapeutic Tissue Engineering Laboratory, Department of Orthopaedic Surgery, National University Health System, National University of Singapore, Singapore
[d] Tissue Engineering Program, Life Sciences Institute, National University of Singapore, Singapore
[e] Department of Surgery, Yong Loo Lin School of Medicine, National University of Singapore, Singapore

ARTICLE INFO

Article history:
Received 4 August 2017
Received in revised form
17 October 2017
Accepted 21 November 2017
Available online 21 November 2017

Keywords:
Mesenchymal stem cells
Exosomes
Cartilage
Regeneration
Chondrocytes
Macrophages

ABSTRACT

Mesenchymal stem cell (MSC) exosome was previously shown to be effective in repairing critical size osteochondral defects in an immunocompetent rat model. Here we investigate the cellular processes modulated by MSC exosomes and the mechanism of action underlying the exosome-mediated responses in cartilage repair. We observed that exosome-mediated repair of osteochondral defects was characterised by increased cellular proliferation and infiltration, enhanced matrix synthesis and a regenerative immune phenotype. Using chondrocyte cultures, we could attribute the rapid cellular proliferation and infiltration during exosome-mediated cartilage repair to exosomal CD73-mediated adenosine activation of AKT and ERK signalling. Inhibitors of AKT or ERK phosphorylation suppressed exosome-mediated increase in cell proliferation and migration but not matrix synthesis. The role of exosomal CD73 was confirmed by the attenuation of AKT and ERK signalling by AMPCP, a CD73 inhibitor and theophylline, an adenosine receptor antagonist. Exosome-treated defects also displayed a regenerative immune phenotype characterised by a higher infiltration of $CD163^+$ regenerative M2 macrophages over $CD86^+$ M1 macrophages, with a concomitant reduction in pro-inflammatory synovial cytokines IL-1β and TNF-α. Together, these observations demonstrated that the efficient osteochondral regeneration by MSC exosomes was effected through a coordinated mobilisation of multiple cell types and activation of several cellular processes.

© 2017 Elsevier Ltd. All rights reserved.

1. Introduction

Articular cartilage has limited capacity for intrinsic regeneration upon injury, and cartilage lesions, if poorly treated, can lead to osteoarthritis (OA), an inflammatory and degenerative joint disease that affects the entire joint, resulting in pain, deformity and loss of function [1–3].

Current treatment modalities for cartilage injuries including microfracture, mosaicplasty and autologous chondrocyte implantation suffer issues of donor site morbidity and/or inferior fibrocartilage repair [4]. Mesenchymal stem cells (MSCs) with their extensive capacities for proliferation and differentiation into various cell lineages have emerged as a promising cell source for treatment of various degenerative, inflammatory and autoimmune diseases [5]. Human MSCs are currently in clinical trials for treatment of cartilage injuries and OA [6–8]. However, as with all cell-based therapies, MSC-based therapy incurs significant operational costs and challenges as cell-based medicine requires stringently monitored manufacturing and storage to ensure optimal viability and vitality of the cells from harvest, expansion, storage and finally delivery to the patient [4].

Although the use of MSCs for tissue repair such as cartilage repair was first predicated on the hypothesis that these cells could differentiate into chondrocytes to replace the damaged tissue, it is now widely accepted that MSCs secrete factors to promote tissue repair [9–11]. In corroboration with this hypothesis, co-culture

* Corresponding author. Faculty of Dentistry, National University of Singapore, 11 Lower Kent Ridge Road,119083, Singapore.
E-mail address: dentohws@nus.edu.sg (W.S. Toh).

https://doi.org/10.1016/j.biomaterials.2017.11.028
0142-9612/© 2017 Elsevier Ltd. All rights reserved.

studies demonstrated that MSCs secrete factors to promote proliferation and matrix synthesis of chondrocytes [12,13].

Among the numerous trophic factors secreted by MSCs, exosomes have been identified as the principal agent mediating the therapeutic efficacy of MSCs in several disease indications such as myocardial ischemia/reperfusion (I/R) injury, limb ischemia and pulmonary hypertension [14–17]. Exosomes are small, secreted bilipid membrane vesicles of about 40–100 nm that are thought to function primarily as intercellular communication vehicles to transfer bioactive lipids, nucleic acids (mRNAs and microRNAs) and proteins between cells to elicit biological responses in recipient cells [15]. We have previously reported that human MSC exosome was efficacious in repairing critical size osteochondral defects in rats [18]. In this study to investigate the mechanism underlying MSC exosome-mediated cartilage repair, we studied the effects of MSC exosomes on chondrocyte survival, migration, proliferation and matrix synthesis, as well as macrophage response and associated cytokine production.

2. Methods

2.1. Preparation of MSC exosomes

Immortalized E1-MYC 16.3 human embryonic stem cell-derived MSCs were cultured in Dulbecco's Modified Eagle's Medium (DMEM) with 10% fetal bovine serum (FBS), as previously described [19,20]. For exosome preparation, the cells were grown in a chemically defined medium for 3 days and exosomes were purified from the conditioned medium (CM) as previously described [14]. The conditioned medium was size fractionated and concentrated 50 × by tangential flow filtration using a membrane with a molecular weight cut-off (MWCO) of 100 kDa (Sartorius, Gottingen, Germany), and assayed for protein using a NanoOrange Protein Quantification Kit (Life Technologies). Each batch of exosome preparation was ascertained to have similarly sized particles with a modal size of 100 nm, a flotation density of 1.10–1.19 g/ml, and presence of exosome-associated markers including CD81, ALIX and TSG101 [14,18]. The exosomes were filtered with a 0.22 μm filter (Merck Millipore, Billerica, MA, USA) and stored in −20 °C freezer until use.

2.2. Chondrocyte isolation and culture

Primary chondrocytes were harvested from knee and hip articular cartilage of 8-week old Sprague Dawley (SD) female rats, following the procedure previously described [21]. Briefly, the cartilage tissues were washed 3 times with phosphate-buffered saline (PBS) and digested with 0.2% collagenase II (Worthington, Lakewood, NJ, USA) overnight at 37 °C. The cells were then passed through the 40-μm cell strainer (Corning®, Corning, NY, USA) to disperse the cells into single cells before seeding at a density of 2×10^4 cells/cm^2. The culture was maintained in DMEM-F12 supplemented with 10% FBS, 25 μg/ml ascorbic acid 2-phosphate (AA2P, Sigma, St. Louis, MO, USA), and 1% penicillin-streptomycin (PS; Life Technologies, Carlsbad, CA, USA) under a humidified atmosphere of 5% CO_2 at 37 °C. The medium was changed every alternate day. Upon confluency, chondrocytes were dissociated using TrypLe (Life Technologies) and further sub-cultured to passage 2 (P2) cells for *in vitro* experiments.

2.3. Exosome treatment and inhibitor study

P2 chondrocytes were seeded at a density of 2×10^4 cells/cm^2, and cultured for 16 h before the medium was changed to a low serum culture medium comprising of DMEM-F12 supplemented with 0.5% FBS and 1% PS for 24 h, and then treated with varying concentrations of exosomes or the vehicle (PBS) as control for over 3 days. To investigate the involvement of adenosine and activation of AKT and ERK pathways, chondrocytes were pre-treated with 1 mM theophylline (a non-selective adenosine receptor antagonist; Sigma) [22], 1 μM wortmannin (AKT inhibitor) or 10 μM U0126 (ERK inhibitor) (Cell Signalling Technology, Danvers, MA, USA) for 1 h, before treatment with exosomes for over 48 h. In experiment with CD73 inhibitor, adenosine 5′-(α,β-methylene)diphosphate (AMPCP) (Sigma), cells were co-treated with exosomes and 200 μM AMPCP for 2 h. Following treatment, chondrocytes were rinsed with PBS and subjected to further analysis. All *in vitro* experiments were performed in triplicates ($n = 3$) in at least two independent experiments.

2.4. Cellular uptake of exosomes

Exosomes were first labelled with Alexafluor 488 dye using a protein labelling kit (Life Technologies) according to the manufacturer's instruction. Briefly, 100 μg exosomes were incubated with 100 μl dye reaction mixture of 10 μl of Alexafluor 488 dye and 10 μl of 1 M sodium carbonate (pH 8.3) in PBS. The reaction mixture was incubated for 1 h at room temperature before transferred into Biospin P6 gel column and centrifuged at 1000 *g* for 4 min to remove the free dye. Rat chondrocytes were incubated with 10 μg/ml of Alexafluor 488-labelled exosomes and observed at 1, 3, 12 and 24 h to determine the uptake of the labelled exosomes by confocal microscopy (FV300, Olympus, Tokyo, Japan). In some experiments, labelling of chondrocytes with CellTracker™ Red CMTPX dye (Thermo Fisher Scientific) was performed.

2.5. Cell proliferation

Cells were seeded at 5000 cells/well in 96-well plates and treated with 1, 5 and 10 μg/ml of exosomes or vehicle control (PBS). At 2, 24, 48 and 72 h, cell metabolic activity and total DNA content were measured. Cell metabolic activity was measured using the MTS (3-(4,5-dimethylthiazol-2-yl)-5-(3-carboxymethoxyphenyl)-2-(4-sulfophenyl)-2H-tetrazolium) assay kit (Promega, Madison, WI, USA) following the manufacturer's specifications. 20 μl of MTS reagent was added to each well and incubated at 37 °C for 2 h. Absorbance readings were then taken at 490 nm and 650 nm (reference) using a microplate reader (Infinite® 200 PRO, Tecan™, Männedorf, Switzerland). Total DNA content that is reflective of cell number was measured, as previously described [23]. Briefly, the cells were lysed by adding 50 μl CelLytic M cell lysis buffer (Sigma) to each well, and DNA concentration was measured using the Quant-iT™ Picogreen® dsDNA assay kit (Life Technologies) according to the manufacturer's instructions. The fluorescence readings were then taken at excitation 480 nm and emission 520 nm using the microplate reader (Infinite® 200 PRO, Tecan™).

2.6. Cell migration

The migration of chondrocytes in response to exosome treatment was assessed using a Transwell system. Briefly, 5×10^4 cells in 300 μl of low serum culture medium (DMEM-F12 supplemented with 0.5% FBS and 1% PS) were placed in the upper chamber, and 1, 5 or 10 μg/ml exosomes or vehicle control (PBS) were added to the lower chambers. After 16 h, the upper surface of the transwell filters was swabbed free of cells. Cells on the underside of the filter were then fixed in 4% (v/v) paraformaldehyde and stained with haematoxylin and eosin. The cells in five randomly-selected fields at 100X magnification were counted. The percentage of cell migration was calculated by normalizing the number of cells on the

underside of the filter to the initial number of cells seeded, and compared against that of the control which was set at 100%.

2.7. Real-time quantitative PCR

Total RNA was isolated from chondrocyte cultures using PureLink® RNA Mini kit (Thermo Fisher Scientific) according to manufacturer's instructions. The RNA was then reverse transcribed using iScript™ reverse transcription Supermix (Bio-Rad Laboratories, Hercules, CA, USA) and then amplified using CFX Connect™ real-time PCR system (Bio-Rad) with iTaq™ Universal SYBR® Green Supermix (Bio-Rad), and primers, as shown in Table 1. The PCR cycling condition comprised an initial denaturation at 95 °C for 30 s followed by 40 cycles of amplification consisting of a 15 s denaturation at 95 °C and a 30 s extension at 60 °C. Relative mRNA expression levels were normalized against glyceraldehyde 3-phosphate dehydrogenase (*GAPDH*) mRNA, and calculated using the comparative ΔCT method [24], and finally expressed as fold changes.

2.8. Sulfated glycosaminoglycan and DNA quantification

To measure sulfated glycosaminoglycan (s-GAG), samples ($n = 3$) were enzymatically digested as previously described [25]. Briefly, samples were digested with proteinase K digestion buffer (100 μg/ml in Tris-HCl buffer, pH 8) for 18 h at 60 °C. Sulfated GAG was measured using Biocolor Blyscan Glycosaminolgycan Assay Kit (Biocolor Ltd, Carrickfergus, UK), as per manufacturer's instructions [25]. The precipitate was collected by high speed centrifugation at 12,000 *g* and dissolved in the dissociation reagent. The dye in the samples and standards were measured at 656 nm using a microplate reader (Infinite® 200 PRO, Tecan™). The readings were normalized against the DNA content of the samples. DNA was measured using Quant-iT™ Picogreen dsDNA assay kit (Life Technologies).

2.9. Western blot hybridization

Western blot hybridization was performed using standard protocols. Briefly, proteins were denatured, separated on 4–12% polyacrylamide gels (Thermo Fisher Scientific), electro-blotted onto a nitrocellulose membrane (GE Healthcare), probed with primary antibody followed by incubation with horseradish peroxidase (HRP)-coupled secondary antibody against the primary antibody. The primary antibodies used in this study were rabbit anti-AKT1/2/3, mouse anti-ERK1/2 and anti-GAPDH (Santa Cruz Biotech, Dallas, TX, USA) and rabbit anti-phospho-AKT (Ser473) and anti-phospho-ERK1/2 (Thr202/Tyr204) (Cell Signalling Technology). After incubating with the appropriate HRP-coupled secondary antibodies (GE Healthcare), visualization of the protein bands was performed by incubating with SuperSignal West Pico Chemiluminescent Substrate (Thermo Fisher Scientific) and then documented using the ChemiDoc™ MP System (Bio-Rad).

Table 1
Primer sequences used for quantitative RT-PCR.

Gene	Primer sequence	Product size
Survivin	F: AACTGGCCCTTCCTGGAG R: TCAGGCTCATTCTCGGTAG	89 bp
Bcl-2	F: GCCTTCTTTGAGTTCGGTG R: GCCAGGAGAAATCAAACAGAG	199 bp
PCNA	F: CAACTTGGAATCCCAGAACAGGAG R: TAAGGTCCCGGCATATACGTGC	82 bp
FGF-2	F: CGGTACCTGGCTATGAAGGA R: CCAGGCGTTCAAAGAAGAAA	82 bp
TGF-β1	F: AAGAAGTCACCCGCGTGCTA R: TGTGTGATGTCTTTGGTTTTGTCA	70 bp
Sox9	F: CTGAAGGGCTACGACTGGAC R: TACTGGTCTGCCAGCTTCCT	140 bp
COMP	F: TGACTTCGATGCTGACAAGG R: GAACGATCTCCATTCCCTGA	167 bp
COL2A1	F: CCCCTGCAGTACATGCGG R: CTCGACGTCATGCTGTCTCAAG	60 bp
GAPDH	F: GGTCGGTGTGAACGGATTTGG R:GCCGTGGGTAGAGTCATACTGGAAC	148 bp

All procedures were performed according to the Institutional Animal Care and Use Committee at National University of Singapore under protocol number: R14-913. Thirty-six 8-week old SD rats with a mean weight of 212.5 ± 17.1 g (range 180–230 g) were used in this study. Osteochondral defects (1.5 mm diameter and 1 mm depth) were created on the trochlear grooves of the distal femurs of these rats with a drill bit, as previously described [26]. The joint capsule and overlying muscle were then closed with suture. The animals were randomly allocated to two groups: defects treated with 100 μg exosomes ($n = 36$) and contralateral control defects treated with PBS vehicle ($n = 36$). Intra-articular injections of exosomes (100 μg exosomes per 100 μl of injection) or PBS vehicle control (100 μl) were administered immediately after the surgery and subsequently on a weekly basis. Animals were housed individually and allowed to move without restriction. Standard food and water were provided *ad libitum*. At 2, 6 and 12 weeks, animals were euthanized by CO_2 inhalation. Distal femora and synovium tissue samples were harvested for analysis. Samples of synovial fluid were also collected for assay of cytokine production.

2.10. Rat osteochondral defect model

2.11. Histology and immunohistochemistry

Tissue samples were fixed in 10% (v/v) neutral buffered formalin (Sigma) overnight and decalcified in 30% (v/v) buffered formic acid. After decalcification, the samples were dehydrated and embedded in paraffin. Serial sections were cut at 5-μm and were stained with haematoxylin and eosin (HE) to examine the morphology and with safranin-O/fast green (Saf-O) to examine s-GAG deposition. Immunohistochemistry was performed as previously described [27] to detect cartilage matrix proteins (type I, II and VI collagens), proliferating cells (proliferative cell nuclear antigen, PCNA), apoptotic cells (cleaved caspase-3, CCP3), and macrophages (CD86 and CD163). CD86 was assessed as a marker for M1 macrophages [28], and CD163 as marker for M2 macrophages [29]. The list of antibodies used in immunohistochemistry is summarized in Table 2. For semi-quantitative analysis of type I and II collagens, the percentage of positively-stained area in the estimated cartilage layer in the defect area was analysed using ImageJ software (National Institutes of Health, Bethesda, MD, USA). Positively-stained cells with distinct pericellular staining of type VI collagen in the cartilage layer in the defect area were counted at 200X

Table 2
Antibodies used for immunohistochemistry.

Antibody	Clone	Dilution	Company
Type II collagen	Mouse 6B3	1:500	Chemicon
Type I collagen	Mouse COL-1	1:1000	Sigma
Type VI collagen	Rabbit polyclonal	1:6000	Abcam
PCNA	Mouse PC10	1:10000	Abcam
Cleaved caspase-3 (CCP3)	Rabbit Asp175	1:300	Cell Signalling
CD163	Mouse ED2	1:100	Bio-Rad
CD86	Rabbit EP1158Y	1:100	Abcam

Table 3
Histological grading scale for cartilage repair.

Category	Points
Cell morphology	
Hyaline cartilage	0
Mostly hyaline cartilage	1
Mostly fibrocartilage	2
Mostly non-cartilage	3
Non-cartilage only	4
Matrix-staining (metachromasia)	
Normal (compared with host adjacent cartilage)	0
Slightly reduced	1
Markedly reduced	2
No metachromatic stain	3
Surface regularity[a]	
Smooth (>3/4)	0
Moderate (>1/2–3/4)	1
Irregular (1/4–1/2)	2
Severely irregular (<1/4)	3
Thickness of cartilage[b]	
>2/3	0
1/3–1/2	1
<1/3	2
Integration of donor with host adjacent cartilage	
Both edges integrated	0
One edge integrated	1
Neither edge integrated	2
Total maximum	14

[a] Total smooth area of the reparative cartilage compared with the entire area of the cartilage defect.
[b] Average thickness of the reparative cartilage compared with that of the surrounding cartilage.

magnification, and expressed as mean number of cells per area (mm^2) [27]. The histologic grading scale described by Wakitani [30] was used to evaluate the quality of the repaired tissue (Table 3) by two independent blinded observers. The score ranges from 0 to 14. A score of 0 indicates normal cartilage, with higher scores indicating progressively more severe damage. For quantification analysis of PCNA, CCP3, CD86 and CD163, positively-stained cells were counted in three randomly-selected fields at 200X magnification, and expressed as mean number of cells per high power field (cells/HPF).

2.12. Multiplex cytokine assay

Pro-inflammatory cytokines including interleukin (IL)-1β, IL-6, and tumour necrosis factor (TNF)-α present in the synovial fluid samples were measured using the Bio-Plex® Multiplex Immunoassay (Bio-Rad) following the manufacturer's instructions.

2.13. Statistical analysis

All quantitative data were reported as mean ± standard error of the mean (SEM). Student's t-test or one-way analysis of variance (one-way ANOVA) followed by Scheffe's *post-hoc* test were performed for normally distributed data, and Mann-Whitney test was performed for non-normal data using SPSS version 22.0 (SPSS, Chicago, IL, USA). Statistical significance was set as $P < 0.05$.

3. Results

3.1. MSC exosomes mediate a dynamic remodelling process to accelerate cartilage repair

We had previously reported the efficacy of MSC exosomes in the repair and regeneration of osteochondral defects at 6 and 12 weeks [18]. To better understand the kinetics of this repair, we repeated the study using more rats and included an earlier time point of 2 weeks (Fig. 1A). In this study, we observed that the exosomes initiated repair of critical size osteochondral defects as early as 2 weeks with significantly more neotissue formation and extracellular matrix (ECM) deposition of s-GAG and type II collagen (Fig. 1B, D–F). Percentage areal deposition of type II collagen was significantly higher in exosome-treated defects than in PBS-treated defects (29.9 ± 4.3 *vs.* 14.8 ± 2.4%; $P = 0.005$) (Fig. 1I). Consistent with this, the exosome-treated group had a better Wakitani score of 8.3 ± 0.8 than the score of 11.4 ± 0.6 in the control group ($P = 0.007$, Fig. 1C).

The enhanced tissue repair in the exosome-treated animals at 2 weeks persisted and extended to week 6 and 12. At 6 weeks, exosome-treated defects showed improved surface regularity and integration with the host cartilage while the control defects displayed poor surface regularity with structure disruptions and fissures (Fig. 1B). Histologically, exosome-treated reparative tissue showed predominately hyaline cartilage formation characterised by presence of chondrocytic cells (*i.e.* spherical with lacuna) and high expression of s-GAG and type II collagen, and low expression of type I collagen (Fig. 1D–G). Hypertrophic chondrocytes with enlarged lacuna were observed in the deep zone of the subchondral bone. In contrast, PBS-treated defects showed mostly fibrous tissue that stained diffusely for type I and VI collagens, but not for s-GAG and type II collagen. By means of semi-quantitative image analysis, exosome-treated defects displayed significantly higher percentage areal deposition of type II collagen (55.4 ± 4.9 *vs.* 35.8 ± 2.6%; $P = 0.002$) and lower percentage areal deposition of type I collagen (29.0 ± 2.2 *vs.* 56.7 ± 1.7%; $P < 0.001$) than that of the PBS-treated defects (Fig. 1I and J). At 6 weeks, exosome-treated group improved their Wakitani score by 3.0 to 5.2 ± 0.9, while the control group improved their score by 2.3 to 9.1 ± 0.6 ($P = 0.002$, Fig. 1C).

By 12 weeks, the exosome-treated group showed complete integration with adjacent host cartilage with a smooth surface regularity while the control group showed incomplete neotissue filling with surface irregularity and distinct border areas (Fig. 1B). The regenerated hyaline cartilage in the exosome-treated group composed mainly type II collagen (76.6 ± 3.3%) and minimally type I collagen (30.8 ± 4.7%), and exhibited good structural integration to the adjacent host cartilage supported by complete regeneration of subchondral bone (Fig. 1D–G, I and J). Approximately 814.3 cells/mm^2 appeared chondrocytic and displayed distinct pericellular matrix staining of type VI collagen (Fig. 1H and K). On the other hand, the control group only had fibrous repair tissues that stained faintly for type II collagen (31.7 ± 2.6%) but more intensely for type I collagen (55.2 ± 4.2%) (Fig. 1G and J). At high magnification, cells in the fibrous tissue showed perfused territorial and inter-territorial distribution of type VI collagen and less than 336.6 cells/mm^2 displayed a pericellular localization (Fig. 1H and K). By the end of 12 weeks, the exosome-treated group exhibited a significantly lower score of 2.3 ± 0.7 relative to 7.2 ± 0.9 in the control group ($P < 0.001$, Fig. 1C).

From this study, we conclude that consistent with our earlier report, MSC exosomes not only improve the quality of osteochondral repair [18], it also elicited an earlier and more robust response as evidenced by the significant improvement in Wakitani scores of exosome-treated rats at 2, 6 and 12 weeks against that of the control group. The improvement in the Wakitani scores from 2 to 6 weeks and 6 to 12 weeks were 3.0 ($P = 0.045$) and 3.0 ($P = 0.047$) respectively in the exosome-treated animals, as opposed to 2.3 ($P = 0.11$) and 2.0 ($P = 0.17$) respectively in the PBS-treated animals, further implying that MSC exosomes accelerated tissue repair.

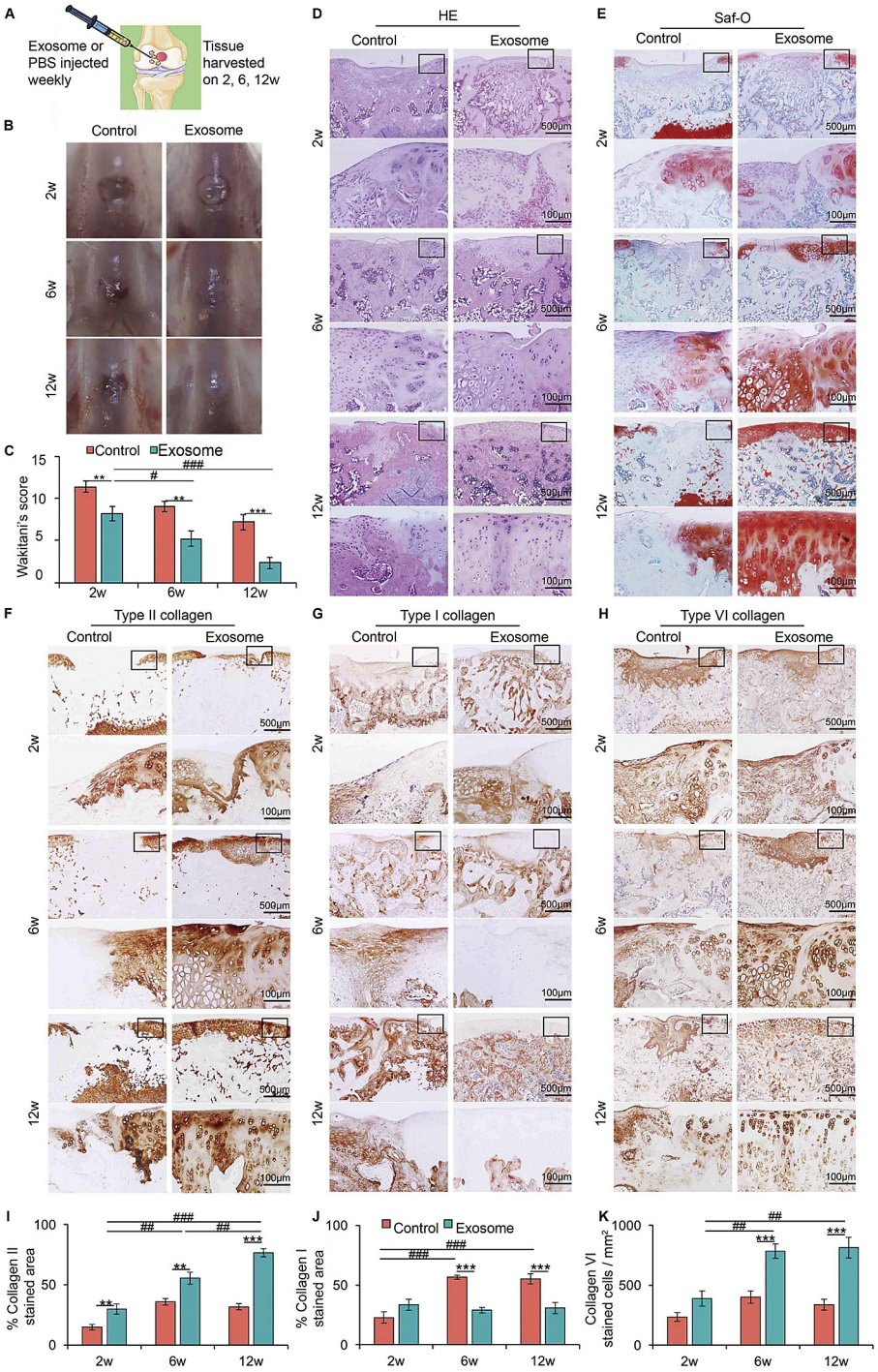

Fig. 1. Macroscopic and histologic evaluation of cartilage repair by MSC exosomes. (A) SD rats were randomly allocated into two groups (Exosome and PBS control; $n = 36$ per group). Intra-articular injections of exosomes (100 μg/100 μl PBS) or vehicle control (100 μl PBS) were administered weekly for up to 12 weeks. At specific time-points (2, 6 and 12 weeks), samples were harvested. (B) Macroscopic evaluation of cartilage repair. (C) Wakitani scores for the histological sections. Data represent mean ± SEM. $^{**}P < 0.01$, $^{***}P < 0.001$ compared to control ($n = 12$). There was also significant improvement in scores of exosome-treated group at 6 weeks ($^{\#}P < 0.05$) and 12 weeks ($^{\#\#\#}P < 0.001$), compared to 2 weeks. Histological analysis of cartilage repair by haematoxylin and eosin (HE) (D), safranin O/fast green (Saf-O) (E), type II collagen (F), type I collagen (G), and type VI collagen (H). Representative images ($n = 12$). Semi-quantitative analysis of immunohistochemical staining. Percentage areal deposition of type II collagen (I) and type I collagen (J), and number of cells with pericellular staining of type VI collagen per mm^2 (K). Data represent mean ± SEM. $^{*}P < 0.05$, $^{**}P < 0.01$, $^{***}P < 0.001$ compared to control ($n = 12$). There was also significant increase in percentage areal deposition of type II collagen in exosome-treated group at 6 weeks ($^{\#\#}P < 0.01$) and 12 weeks ($^{\#\#\#}P < 0.001$), compared to 2 weeks.

3.2. MSC exosomes enhance proliferation and reduce apoptosis during cartilage repair

In parallel to the initiation of significant osteochondral repair at 2 weeks, exosome-treated group also displayed a significant increase in $PCNA^+$ cells compared to that of control group in both the cartilage tissue (232.8 ± 28.0 *vs.* 126.1 ± 21.4 cells/HPF; $P = 0.006$) and in the overlying synovium (115.1 ± 16.8 *vs.* 69.2 ± 8.7 cells/HPF; $P = 0.024$) (Fig. 2A–D). At 6 weeks, the number of $PCNA^+$ cells declined in both treatment and control groups but

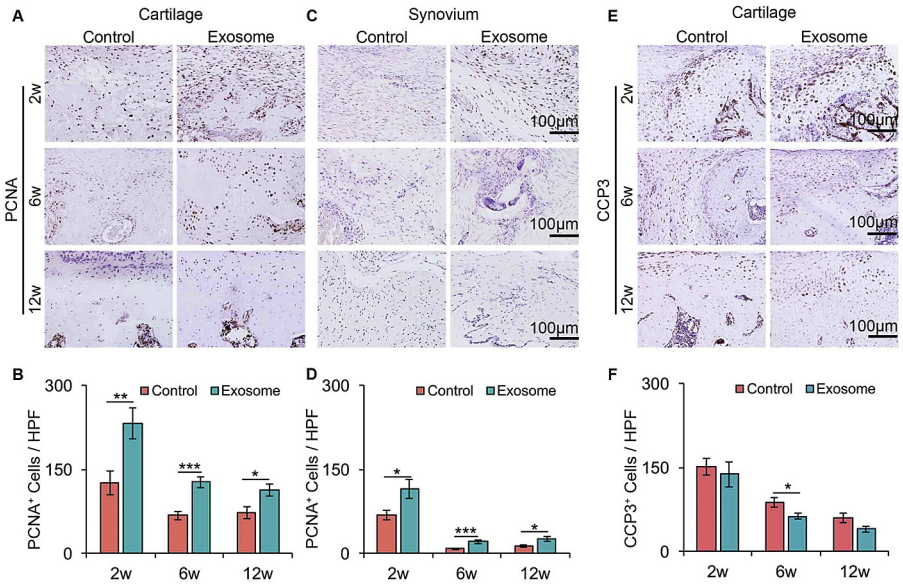

Fig. 2. Evaluation of cellular proliferation and apoptosis during course of cartilage repair. PCNA staining and quantitative analysis of PCNA$^+$ cells on reparative cartilage (A, B) and synovium (C, D) at 2, 6 and 12 weeks. Number of PCNA$^+$ cells was counted per high power field (HPF) at 200X magnification. (E) Cleaved caspase-3 (CCP3) staining and (F) quantitative analysis of CCP3$^+$ cells on reparative cartilage. Number of CCP3$^+$ cells was counted per HPF at 200X magnification. Representative images ($n = 12$). Data represent mean ± SEM. $^*P < 0.05$, $^{**}P < 0.01$, $^{***}P < 0.001$ compared to control ($n = 12$). Scale bar: 100 μm.

remained significantly higher in the exosome-treated group compared to the control group in both the cartilage (127.8 ± 9.6 *vs.* 68.0 ± 7.7 cells/HPF; $P < 0.001$) and in the synovium (21.2 ± 2.6 *vs.* 8.2 ± 1.5 cells/HPF; $P < 0.001$) (Fig. 2A–D). This significantly higher number of PCNA$^+$ cells in both tissues of the exosome-treated group over the control group persisted to week 12. By the end of 12 weeks, the relative distribution of PCNA$^+$ cells between exosome-treated and control groups in the cartilage was 112.4 ± 10.9 *vs.* 73.0 ± 10.7 cells/HPF ($P = 0.017$) and in the overlying synovium was 26.1 ± 4.8 *vs.* 13.3 ± 3.1 cells/HPF ($P = 0.038$) (Fig. 2A–D).

The increase in PCNA$^+$ cells in the cartilage lesion at 2 weeks was paralleled by a similar early increase in CCP3$^+$ apoptotic cells (Fig. 2E–F). The number of CCP3$^+$ cells in both exosome-treated and control groups was 138 ± 22.6 and 150.5 ± 14.9 cells/HPF respectively ($P = 0.652$). However, unlike the PCNA$^+$ cells, CCP3$^+$ apoptotic cell number decreased at 6 weeks with significantly less CCP3$^+$ apoptotic cells in the exosome-treated group compared to the control group (62.6 ± 5.0 *vs.* 88.5 ± 8.7 cells/HPF; $P = 0.019$). By 12 weeks, the number of CCP3$^+$ cells in both exosome-treated and control groups was low (<60 cells/HPF) with no significant difference. Together these observations demonstrated that MSC exosomes enhanced cellular proliferation and attenuated apoptosis.

3.3. MSC exosomes increase M2 macrophage infiltration with a concomitant decrease in M1 macrophages and inflammatory cytokines

Since immune activity is an integral component of tissue injury and repair, we next investigated if the reparative activity of MSC exosomes involves an immune component. Specifically, we investigated if there was a difference in the M1 and M2 macrophage infiltration into exosome- and PBS-treated defects.

We observed an abundance of M2 macrophages as indicated by CD163$^+$ cells in both cartilage and synovium (Fig. 3A–D) as early as 2 weeks. Relative to the control, the exosome-treated defects displayed significantly higher numbers of CD163$^+$ cells in the cartilage (176.9 ± 30.3 *vs.* 80.4 ± 13.3 cells/HPF; $P = 0.008$) and in the overlying synovium (160.0 ± 12.1 *vs.* 106.1 ± 5.1 cells/HPF; $P = 0.001$). Thereafter, the numbers of CD163$^+$ cells declined in both groups but those in the exosome-treated group remained consistently higher than that in the control group.

In contrast to the M2 macrophages, M1 macrophages as indicated by CD86$^+$ cells were reduced in both cartilage and synovium of exosome-treated group compared to the control group (Fig. 3E–H). This exosome-associated reduction in M1 macrophages persisted throughout the 12-week observation. By the end of 12 weeks, exosome-treated group displayed significantly lower numbers of CD86$^+$ cells compared to that of control group in both cartilage reparative tissue (28.8 ± 3.5 *vs.* 63.5 ± 7.2 cells/HPF; $P < 0.001$) and in the overlying synovium (37.6 ± 4.3 *vs.* 82.6 ± 12.9 cells/HPF; $P = 0.006$).

The reduced M1 macrophages in exosome-treated animals was consistent with the significantly lower levels of M1-associated cytokines, IL-1β, and TNF-α (Fig. 3I) in their synovial fluid samples relative to that of PBS-treated animals at 6 weeks ($P < 0.05$). However, the level of IL-6, another M1-associated cytokine was not significantly different in the synovial fluid of exosome- and PBS-treated animals at all time-points.

3.4. Exosome uptake and effects on chondrocyte migration, proliferation and matrix synthesis

As the exosome-mediated regeneration of the cartilage defect was characterised by increased chondrocyte migration, proliferation and matrix synthesis, we tested if these processes were directly modulated by MSC exosomes (Fig. 4A).

To assess if MSC exosomes interact directly with chondrocytes, chondrocytes were incubated with labelled exosomes and monitored by confocal microscopy imaging over 24 h. We observed that the cells rapidly endocytosed the exosomes and became fluorescent within an hour and reached a maximum fluorescent intensity at 12 h (Fig. 4B). At a higher magnification, the labelled exosomes were found mainly localized in cytoplasm of the cell (Fig. 4C). These results implied that MSC exosomes have the potential to communicate directly and rapidly with chondrocytes. In addition, we also

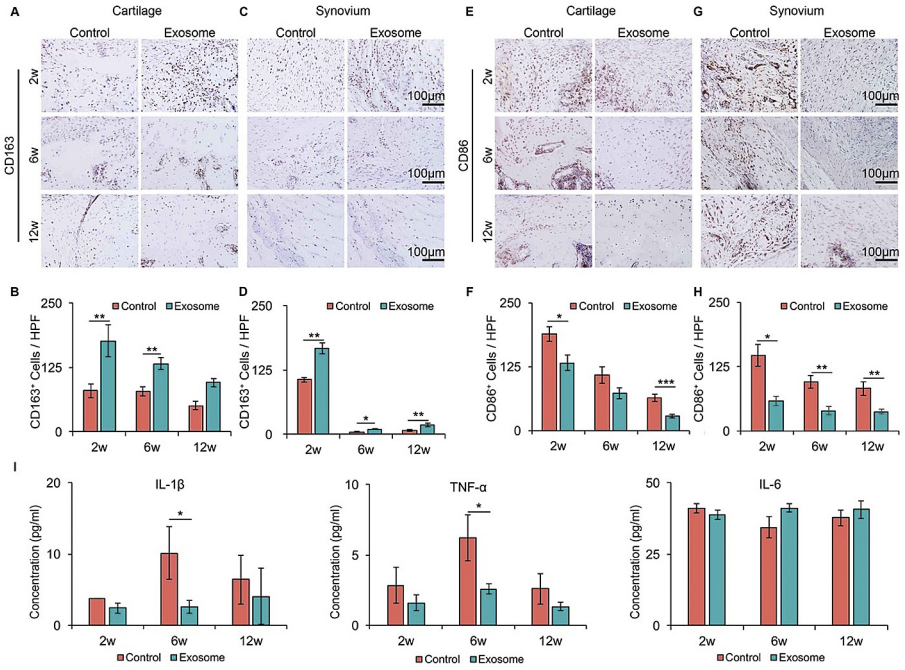

Fig. 3. Effects of MSC exosomes on macrophage infiltration and pro-inflammatory cytokine production during course of cartilage repair. Immunohistochemical staining of CD163 (A–D) and CD86 (E–H) and quantitative analyses of $CD163^+$ and $CD86^+$ cells on reparative cartilage and synovium at 2, 6 and 12 weeks. Representative images ($n = 12$). Scale bar: 100 μm. $CD163^+$ and $CD86^+$ cells were counted per high power field (HPF) at 200X magnification. Data represent mean ± SEM. $^*P < 0.05$, $^{**}P < 0.01$, $^{***}P < 0.001$ compared to control ($n = 12$). (I) Analysis of cytokine production in synovial fluid samples in control and exosome-treated groups. Data represent mean ± SEM. $^*P < 0.05$ compared to control ($n = 1$–6).

observed that when incubated with MSC exosomes, chondrocytes exhibited enhanced migration in a dose-dependent manner. At 10 μg/ml, exosomes induced a 2-fold higher migration rate than that of control ($P < 0.001$, Fig. 4D). Thus, MSC exosomes have the potential to elicit the rapid migration of chondrocytes into the defect as observed during the osteochondral repair in the animal model.

To determine if MSC exosomes affect the proliferation of chondrocytes as observed in the animal model, chondrocytes were treated with increasing concentrations of exosomes over 72 h. Metabolic activity was monitored by MTS assay while proliferation was assessed by measurement of total DNA content. MSC exosomes significantly enhanced metabolic activity in a dose-dependent manner as early as 2 h at 10 μg/ml ($P < 0.01$, Fig. 4E). At 1 and 5 μg/ml, this enhancement was delayed to 24 h ($P < 0.001$, Fig. 4E). By the end of 72 h, chondrocytes treated with 10 μg/ml exosomes demonstrated at least 1.5-fold higher metabolic activity than the control ($P < 0.001$, Fig. 4E).

As with metabolic activity, DNA content which is reflective of the cell number increased with increasing concentrations of exosomes (Fig. 4E). Similar to metabolic activity, significant differences in cell numbers between exosome treatment group and control were observed after 4 h. From 24 h onwards, 5 and 10 μg/ml of exosome induced a significant dose-dependent increase in cell numbers compared to the control ($P < 0.01$). By the end of 72 h, chondrocytes in the 10 μg/ml exosome treatment group proliferated ~2-fold faster than those in the control ($P < 0.001$, Fig. 4E).

As chondrocyte proliferation is often associated with dedifferentiation that results in loss of chondrocytic phenotype and decreased potential for matrix synthesis [31], we determined if the induction of chondrocyte proliferation by MSC exosomes would result in the loss of matrix biosynthesis. Specifically, we assayed for s-GAG synthesis during exosome-treatment of chondrocytes. At 24 and 72 h after exosome treatment, the levels of s-GAG ($P < 0.01$) and s-GAG/DNA ($P < 0.05$) were significantly increased in comparison to those treated with PBS (Fig. 4F).

All the above findings were further supported by our gene expression analysis. Genes associated with chondrocyte survival and proliferation such as *Survivin*, *Bcl-2*, *FGF-2* and *PCNA* were significantly increased at mRNA levels within 24 h of exposure to 10 μg/ml exosomes ($P < 0.05$, Fig. 4G). In addition, FGF-2 which is also a chemotactic factor of chondrocytes [32] was robustly upregulated at 4 h (Fig. 4G), providing a temporally relevant molecular rationale for exosome-mediated enhancement of cell migration at 16 h. Consistent with our earlier finding of elevated s-GAG levels, we found that MSC exosomes enhanced the expression of several genes associated with chondrogenic differentiation and matrix synthesis. Among these genes, we observed significant increase in mRNA levels of chondrogenic factor - TGF-β1 at 4 h ($P = 0.04$), and cartilage matrix proteins - COMP at 72 h ($P = 0.05$) and COL2A1 at 24 and 72 h ($P < 0.05$) compared to the control. However, the mRNA level of Sox9 was marginally increased at 72 h by exosome treatment but was not significantly different compared to the control (Fig. 4G).

3.5. MSC exosomes modulate chondrocyte functions through adenosine-mediated activation of AKT and ERK signalling pathways

As the first significant cellular response to exosome (*i.e.* cellular proliferation) was detected as early as 24 h and the average mammalian cell cycle is also 24 h [33], MSC exosomes must have elicited this response within minutes of contacting the cells. Therefore, the most likely pathway to elicit such a rapid cellular response is a signal transduction pathway. As AKT and ERK signalling pathways are the major pathways implicated in cellular survival, proliferation and matrix synthesis including those of chondrocytes [34–36], we investigated the effect of exosomes on AKT and ERK signalling in chondrocyte culture. As shown in Fig. 5A, AKT and ERK were rapidly phosphorylated within 1 h and peaked at 6 h. These findings demonstrated that MSC exosomes can activate

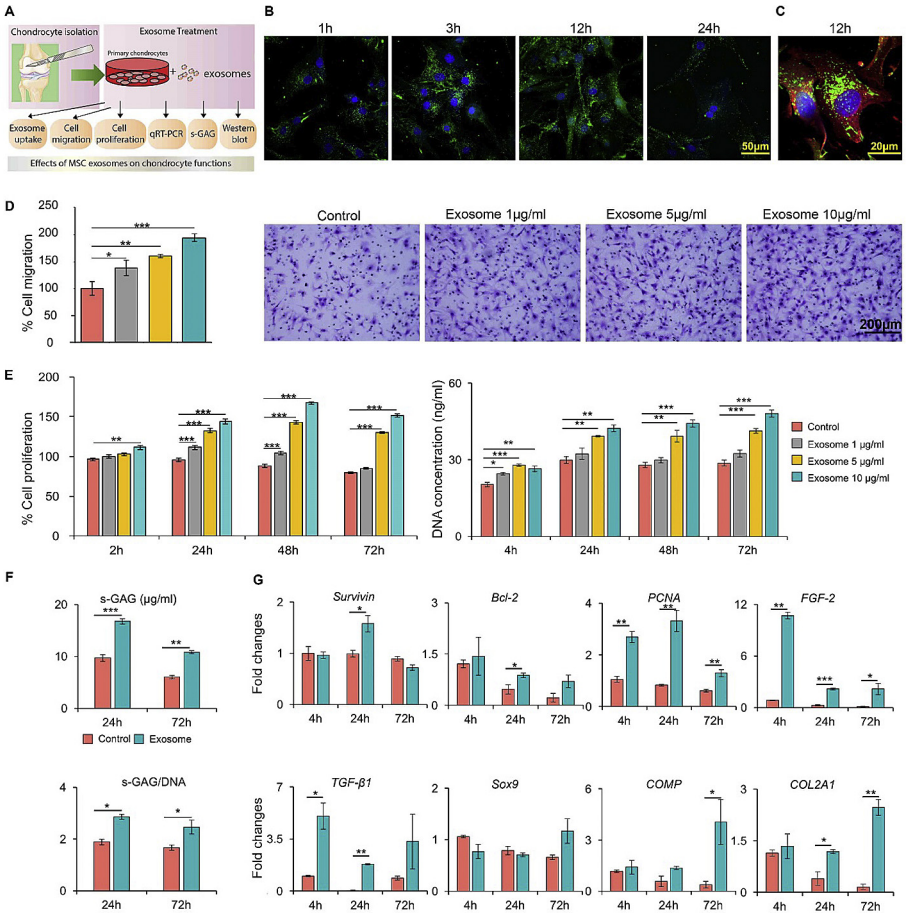

Fig. 4. Effects of MSC exosomes on chondrocyte functions. (A) Experiment design. (B) Cellular uptake assay by confocal microscopy demonstrated rapid uptake of MSC exosomes (green). (C) Merged images of Celltracker Red-labelled chondrocyte (red) and Alexafluor-488-labelled exosomes (green) at high magnification revealed localization of exosomes in the cytoplasm. (D) Transwell migration assay showed dose-dependent effect of MSC exosomes on chondrocyte migration. Data represent mean ± SEM. $^{*}P < 0.05$, $^{**}P < 0.01$, $^{***}P < 0.001$ compared to control ($n = 3$). (E) MTS metabolic assay (left) and DNA assay (right) showed potent dose and time-dependent effects of MSC exosomes on chondrocyte metabolic activity and proliferation. Data represent mean ± SEM. $^{*}P < 0.05$, $^{**}P < 0.01$, $^{***}P < 0.001$ compared to control ($n = 3$). (F) Quantitative analysis of s-GAG (top) and s-GAG/DNA (bottom) showed significant increase in s-GAG production by 10 μg/ml exosome treatment. Data represent mean ± SEM. $^{*}P < 0.05$, $^{**}P < 0.01$, $^{***}P < 0.001$ compared to control ($n = 3$). (G) Quantitative RT-PCR analysis showed regulation of genes associated with anti-apoptosis (*Survivin, Bcl-2*), proliferation (*PCNA, FGF-2*), migration (*FGF-2*) and differentiation (*TGF-β1, Sox9, COMP* and *COL2A1*) by 10 μg/ml exosome treatment. Data represent mean ± SEM. $^{*}P < 0.05$, $^{**}P < 0.01$, $^{***}P < 0.001$ compared to control ($n = 3$). (For interpretation of the references to colour in this figure legend, the reader is referred to the web version of this article.)

the chondrocytes rapidly, correlating directly with the rapid increase in chondrocyte metabolic activity and gene expression.

Next, we investigated the role of AKT and ERK signalling in MSC exosome-mediated promotion of chondrocyte migration, proliferation, and matrix synthesis. As shown in Fig. 5B, phosphorylation of AKT and ERK induced by MSC exosomes was abrogated by wortmannin and U0126. Functionally, MSC exosomes promoted cell migration, but was suppressed by AKT inhibition ($P < 0.001$) and to a lesser extent by ERK inhibition ($P < 0.01$, Fig. 5C). Similarly, MSC exosomes enhanced the proliferation of chondrocytes but this was significantly reduced by inhibition of AKT pathway ($P < 0.05$, Fig. 5D). Interestingly, inhibition of AKT or ERK did not reduce the level of s-GAG production induced by MSC exosomes, suggesting that other pathways might be mediating this process (Fig. 5E). As shown in Fig. 5F, elevated expression of FGF-2 and Survivin induced by MSC exosomes at 24 h post-treatment was partially suppressed by AKT and ERK inhibition. On the other hand, mRNA levels of TGF-β1 and COL2A1 were partially downregulated by AKT (but not ERK) inhibition. However, there were no significant differences in mRNA levels of PCNA and COMP with either AKT or ERK inhibition.

We previously reported that MSC exosome expresses CD73/ecto-5′-nucleotidase that can convert extracellular AMP to adenosine which in turn can elicit pro-survival AKT and ERK signalling via interaction with adenosine receptor [37,38]. Here, we determined if CD73/adenosine pathway is involved in AKT/ERK activation. As previously reported, we first confirmed that MSC exosomes express CD73 (Fig. 6A). In the presence of AMPCP, a CD73 inhibitor, exosome-mediated phosphorylation of AKT and ERK in chondrocytes was attenuated (Fig. 6B). Similarly, phosphorylation of AKT, and lesser extent of ERK, was reduced in the presence of theophylline, a non-selective adenosine receptor antagonist that antagonized the adenosine receptors including A1, A2A, A2B, and A3 receptors (Fig. 6C). Collectively, our findings suggest that MSC exosomes can induce phosphorylation of AKT and also of ERK to a lesser extent through CD73/ecto-5′-nucleotidase activity. As AMPCP and theophylline did not completely abrogate exosome-mediated phosphorylation of AKT and ERK, it is possible that there are other exosome mediators of AKT and ERK phosphorylation.

4. Discussion

MSC therapies have proven to be efficacious for cartilage repair in animal and clinical studies [6,39], but are hampered by logistical

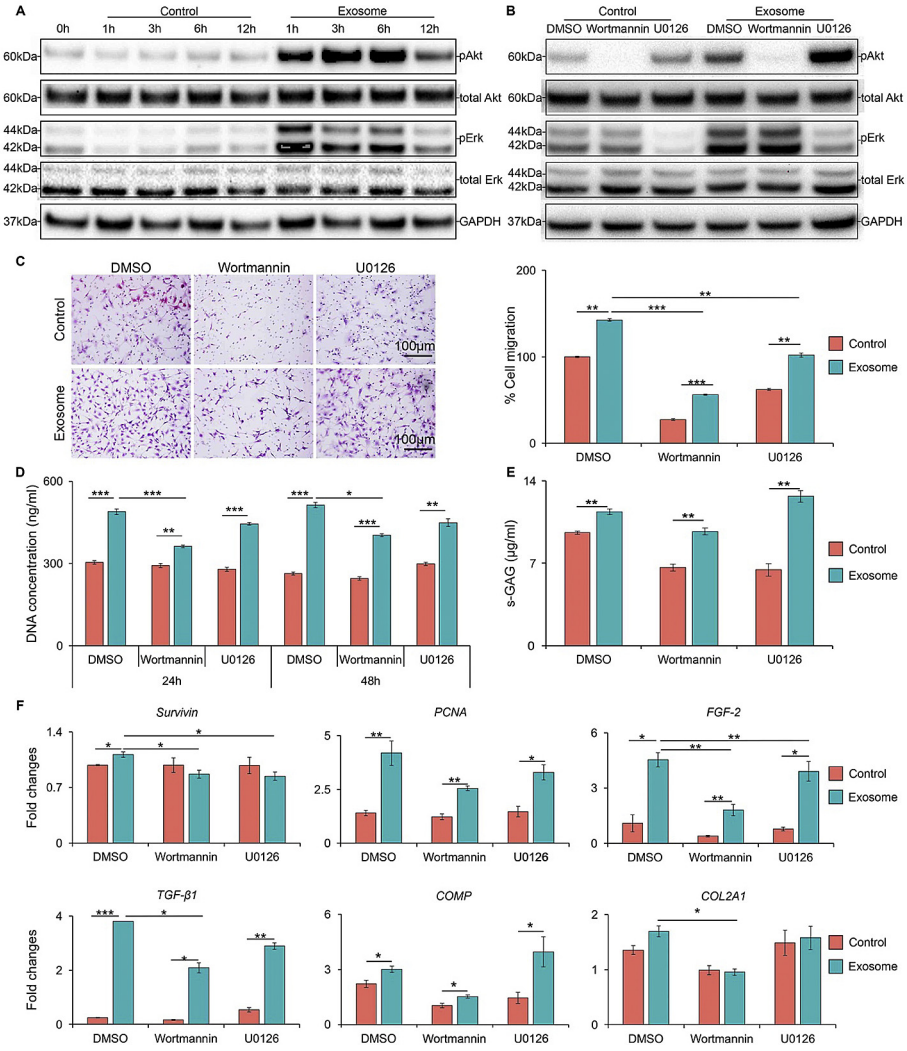

Fig. 5. Exosome-mediated activation of AKT and ERK pro-survival signalling and their effects on chondrocyte functions. (A) Intracellular signalling in chondrocytes after exposure to 10 μg/ml exosome treatment showed activation of AKT and ERK signalling pathways. Representative results of 2 independent experiments. (B) MSC exosomes induced AKT and ERK activation, but these effects were abolished by AKT (wortmannin; 1 μM) and ERK inhibitors (U0126; 10 μM). Representative results of 2 independent experiments. (C) Transwell migration assay showed that exosome-mediated migration of chondrocytes was suppressed by AKT and ERK inhibition. Data represent mean ± SEM. $^{**}P < 0.01$, $^{***}P < 0.001$ ($n = 3$). (D) DNA assay showed that MSC exosomes enhanced chondrocyte proliferation, but these effects could be reversed by inhibition of AKT signalling pathway. Data represent mean ± SEM. $^{*}P < 0.05$, $^{**}P < 0.01$, $^{***}P < 0.001$ ($n = 3$). (E) Level of s-GAG production was enhanced by exosome treatment, but this effect was not suppressed by AKT or ERK inhibition. Data represent mean ± SEM. $^{**}P < 0.01$ ($n = 3$). (F) Quantitative RT-PCR analysis at 24 h post-treatment showed involvement of AKT and ERK signalling pathways in exosome-mediated regulation of genes associated with anti-apoptosis (*Survivin*), proliferation (*PCNA*, *FGF-2*), migration (*FGF-2*) and differentiation (*TGF-β1*, *COMP* and *COL2A1*). Data represent mean ± SEM. $^{*}P < 0.05$, $^{**}P < 0.01$, $^{***}P < 0.001$ ($n = 3$).

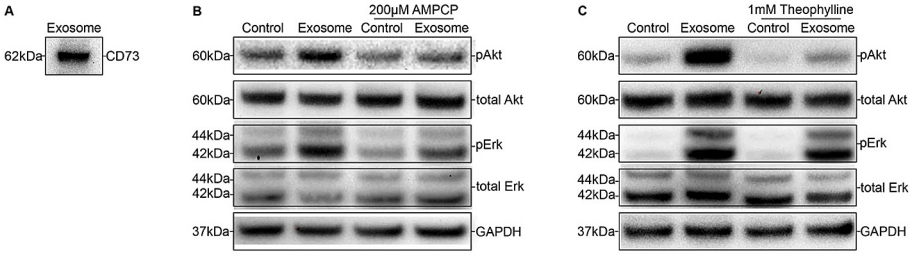

Fig. 6. Exosomes mediated activation of AKT and ERK pro-survival signalling through CD73/ecto-5′-nucleotidase activity. (A) Presence of CD73/ecto-5′-nucleotidase on 22.5 μg MSC exosomes. (B) The addition of CD73 inhibitor (AMPCP; 200 μM) for 2 h reduced AKT and ERK activation. (C) The phosphorylation of AKT, and lesser extent of ERK, was attenuated in the presence of theophylline (1 mM), a non-selective adenosine receptor antagonist. Representative results of 2 independent experiments.

and operational challenges for proper storage and handling of the cells to maintain the cell viability and vitality needed for transplantation [40]. Although the use of MSCs for cartilage repair was predicated on their potential to differentiate into chondrocytes and replace dead or injured chondrocytes, it is increasingly evident that the reparative potential of MSCs is derived from its secretion instead [9,11]. Among the numerous factors present in the MSC secretion, exosome was first identified and reported to be the principal active component underlying the therapeutic efficacy of MSCs against myocardial I/R injury in 2010 [14]. Since then, MSC exosomes were found to be efficacious against many disease targets of MSCs [14–17]. In cartilage regeneration, we had previously reported that MSC exosome effectively repairs critical size osteochondral defects in an immunocompetent rat model [18]. However, the underlying mechanism of action for MSC exosome-mediated cartilage regeneration remains unknown. In this report, we demonstrated in an adult immunocompetent rat model that human MSC exosomes initiate rapid repair and regeneration of osteochondral defects via a multi-faceted mechanism that co-ordinates the modulation of several cellular processes such as migration, proliferation, matrix synthesis, macrophage infiltration and cytokine production for optimal tissue repair (Fig. 7). MSC exosomes derive this potential to execute a co-ordinated multi-faceted mechanism through their large diverse proteomic and RNA cargo [38,41].

In this study, we observed that MSC exosomes initiated neotissue formation and subsequent cartilage repair as early as 2 weeks and this was accompanied by active proliferation and migration of cells as evident by the increased numbers of $PCNA^{+}$ cells in the cartilage defect site and overlying synovium. We hypothesized that MSC exosomes enhanced cartilage repair by inducing migration and proliferation of appropriate reparative cell types such as chondrocytes to the injured tissues and promoting cartilage matrix synthesis. We tested this hypothesis by assessing the effect of MSC exosomes on migration, proliferation, apoptosis, and matrix synthesis of chondrocytes in cell culture. In support of this hypothesis,

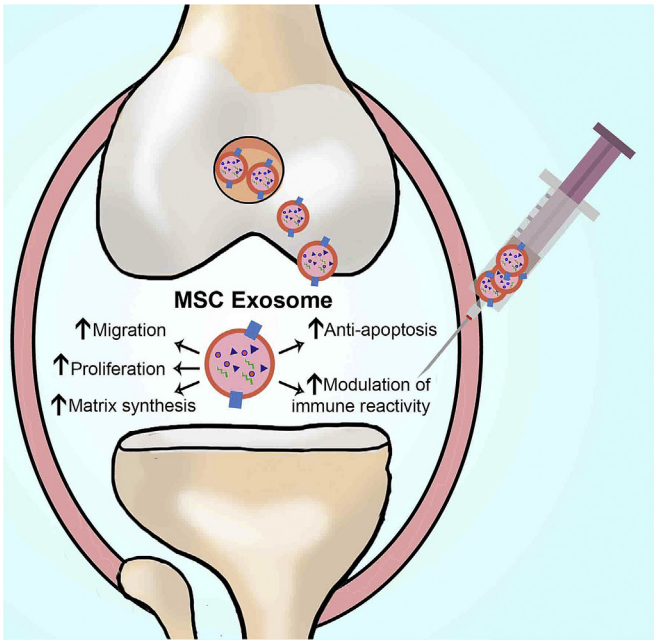

Fig. 7. Proposed underlying mechanisms of MSC exosomes in cartilage regeneration. We propose that MSC exosomes promote cartilage repair and regeneration through a multi-faceted mechanism by enhancing proliferation, migration and matrix synthesis, as well as attenuating apoptosis and modulating immune reactivity.

MSC exosomes were found to increase cell migration, proliferation and matrix synthesis, while simultaneously attenuating apoptosis in chondrocytes *in vitro*. Our observations demonstrated that MSC exosomes have the potential to substantially increase the number of chondrocytes through a synergistic combination of increased proliferation, reduced apoptosis and enhanced recruitment while promoting matrix synthesis. Concomitant with this synergistic combination, we also observed exosome-mediated increases in the expression of genes associated with proliferation (*PCNA* and *FGF-2*) and anti-apoptosis (*Survivin* and *Bcl-2*).

As exosome-induced cellular proliferation was detected as early as 24 h and the average mammalian cell cycle is also 24 h [33], we postulated that MSC exosomes must have elicited this response within minutes of contacting the cells and that receptor-mediated signal transduction via phosphorylation of survival kinases such as AKT and ERK represented the most likely path for this rapid elicitation of cellular proliferation. We confirmed that MSC exosomes could indeed induced rapid phosphorylation of AKT and ERK in chondrocytes within an hour, and that this phosphorylation was critical in inducing cellular migration and proliferation as attenuation of AKT and ERK phosphorylation by wortmannin and U0126 respectively, significantly reduced cell migration and proliferation, but not s-GAG synthesis (Fig. 5). The activation of AKT and/or ERK pro-survival signalling by exosomes has been reported to be an essential pathway in exosome-mediated tissue repair and regeneration, and have been demonstrated in wound healing [42], bone repair [43] and myocardial regeneration following ischemia injury [44]. In chondrocytes, AKT is probably the more important target of MSC exosomes as attenuation of AKT phosphorylation resulted in a greater reduction in cell migration and proliferation.

To identify the upstream activator of AKT phosphorylation, we postulated CD73 as a likely candidate as it is highly abundant and enzymatically active in MSC exosome [37,38]. It is also the only known extracellular ecto-5′-nucleotidase that can convert extracellular adenosine monophosphate (AMP) to adenosine which in turn can elicit pro-survival AKT and ERK signalling via interaction with adenosine receptor. In the presence of AMP, MSC exosomes were shown to activate AKT and ERK phosphorylation in cardiomyocytes through theophylline-sensitive receptor signalling [38]. In this study, we demonstrated that MSC exosome-mediated phosphorylation of AKT and ERK in chondrocytes was mediated by the ecto-5′-nucleotidase activity of CD73 through the use of a CD73 inhibitor, AMPCP and an adenosine receptor antagonist, theophylline. In the presence of AMPCP, AKT and ERK phosphorylation was attenuated. Non-selective blockade of adenosine receptors by theophylline in chondrocytes also abrogated the effects of MSC exosomes on AKT (and lesser extent of ERK) phosphorylation. As exosome-induced phosphorylation of both AKT and ERK was not completely abrogated by AMPCP and theophylline, it is possible that exosome proteins other than CD73 may mediate the exosome-induced phosphorylation of both AKT and ERK. Proteomic analysis of MSC exosomes had previously indicated that the cargo is highly complex and contains several factors such as transforming growth factor (TGF)-β, platelet-derived growth factor (PDGF) and growth differentiation factor (GDF)-5 that could also activate AKT and/or ERK signalling in chondrocytes [37,45–48]. This possible involvement of other signalling pathways suggests that MSC exosome induction of AKT/ERK signalling may be complex with potential cross-talks across multiple signalling pathways.

A significant aspect of MSC exosome-mediated cartilage repair is its capacity to maintain the differentiated phenotype of chondrocytes such as the synthesis of the cartilage matrix. In fact, the synthesis of s-GAG, an important component of the cartilage matrix was increased by exosome treatment. This increase was not mediated by AKT and/or ERK signalling as it was not affected by the

inhibition of either signalling pathways. Enhanced matrix synthesis by MSC exosomes could be mediated by activation of other signalling pathways such as the SMAD pathway [34]. Unlike a previous report where only exosomes from miR-140-5p overexpressing synovial MSCs could enhance matrix synthesis of chondrocytes [49], we showed here that native MSC exosomes could enhance matrix synthesis of chondrocytes without the need for genetic manipulation.

In this study, we also observed that cartilage injury and repair, like most tissue injuries and repairs involves a significant immune component. Following traumatic cartilage injury, it has been shown that inflammatory cytokines including IL-1β, IL-6 and TNF-α, and catabolic factors such as matrix metalloproteinase (MMP)-1 and MMP-13 are rapidly upregulated, resulting in inflammation, chondrocyte apoptosis and cartilage matrix degradation [50]. Anti-inflammatory intervention to ameliorate inflammation has been shown to promote chondrocyte survival and mitigate the risk of development to post-traumatic OA [51]. For example, M1 polarized macrophages in OA synovium tissues were reported to inhibit MSC chondrogenic differentiation via IL-6 *in vitro* [28] while M2 macrophage polarization supported survival of cartilage graft by production of anti-inflammatory IL-10 to suppress adverse inflammation [52]. However, another study reported that anti-inflammatory cytokines (IL-4 and IL-10) did not inhibit TNF-α and interferon (IFN)-γ induced inflammation of OA cartilage explants [53]. Nevertheless, ameliorating inflammation constitutes an important component of cartilage reparative strategies to promote cartilage repair [51,54]. In our study, we found that MSC exosomes induced higher infiltration of $CD163^{+}$ regenerative M2 macrophages rather than the inflammatory $CD86^{+}$ M1 macrophages at the defect site with a concomitant reduction in pro-inflammatory synovial cytokines (IL-1β and TNF-α). This is consistent with the previously reported immunomodulatory property of MSC exosomes [55] that MSC exosomes could induce expression of anti-inflammatory IL-10 and TGF-β1 and attenuate expression of pro-inflammatory IL-1β, IL-6, TNF-α and IL-12P40 in THP-1 monocytes. They also enhance allogeneic graft survival in mice with a concomitant increase in regulatory T cells. However, the mechanistic role of MSC exosome in modulating the immune microenvironment towards a regenerative and less pro-inflammatory phenotype during cartilage repair needs to be further investigated. For example, it would be critical to determine in future studies if MSC exosomes induce greater migration or polarization of M2 macrophages during cartilage repair.

Although this study demonstrated that MSC exosomes are efficacious in cartilage regeneration, there are still some limitations to our study. Multiple injections of exosome performed in our study may not be clinically feasible. In future studies, it would be necessary to determine the bio-availability and bio-distribution of the exosomes following injection into the joint space and to explore if there is a therapeutic window for fewer injections. Furthermore, the minimal effective dose of exosomes needs to be optimized. Last but not least, this is a proof-of-concept study performed in the rat model. Further investigation in a larger animal model such as the rabbit or pig would be needed, where exosomes could be explored in combination with scaffolds for treatment of cartilage defects and osteoarthritis.

5. Conclusion

Osteochondral defects as a result of cartilage injuries affect both the articular cartilage and the subchondral bone tissues, and therefore the repair and regeneration process will require a coordinated temporal and spatial modulation of multiple cell types. Here we showed that MSC exosomes could repair and regenerate critical size osteochondral defects by mounting a coordinated, multi-faceted response of enhancing proliferation, migration and matrix synthesis, attenuating apoptosis and modulating immune reactivity. Our findings provide the rationale for the development of a *next-generation* ready-to-use and cell-free MSC therapeutic that is highly efficacious for the treatment of complex tissue injuries such as the joint injuries, and potentially osteoarthritis [40,56].

Author contributions

S.Z. performed the experiments, acquired, analysed and interpreted the data, and drafted the manuscript. S.J.C. performed the experiments, acquired, analysed and interpreted the data. R.C.L. analysed and interpreted the data, and edited the manuscript. J.H.P.H. analysed and interpreted the data, and edited the manuscript. S.K.L. analysed and interpreted the data, and edited the manuscript. W.S.T. designed the study, analysed and interpreted the data, drafted and edited the manuscript. All authors approved the final version of the manuscript.

Disclosure

SKL holds founder shares in Paracrine Therapeutics Pte Ltd. All other authors have no competing interests to declare.

Acknowledgement

This work was supported by grant from the National University Healthcare System, National University of Singapore (R221000083112 and R221000090112) and National Medical Research Council Singapore (R221000080511). RCL and SKL are supported by a core grant from A*STAR BMRC.

References

[1] R.F. Loeser, S.R. Goldring, C.R. Scanzello, M.B. Goldring, Osteoarthritis: a disease of the joint as an organ, Arthritis Rheum. 64 (6) (2012) 1697–1707.
[2] M. Marcacci, G. Filardo, E. Kon, Treatment of cartilage lesions: what works and why? Injury 44 (Suppl 1) (2013) S11–S15.
[3] W.S. Toh, M. Brittberg, J. Farr, C.B. Foldager, A.H. Gomoll, J.H. Hui, J.B. Richardson, S. Roberts, M. Spector, Cellular senescence in aging and osteoarthritis, Acta Orthop. 87 (sup363) (2016) 6–14.
[4] Y.Z. Jiang, S.F. Zhang, Y.Y. Qi, L.L. Wang, H.W. Ouyang, Cell transplantation for articular cartilage defects: principles of past, present, and future practice, Cell Transpl. 20 (5) (2011) 593–607.
[5] M.F. Pittenger, A.M. Mackay, S.C. Beck, R.K. Jaiswal, R. Douglas, J.D. Mosca, M.A. Moorman, D.W. Simonetti, S. Craig, D.R. Marshak, Multilineage potential of adult human mesenchymal stem cells, Science 284 (5411) (1999) 143–147.
[6] H. Nejadnik, J.H. Hui, E.P. Feng Choong, B.C. Tai, E.H. Lee, Autologous bone marrow-derived mesenchymal stem cells versus autologous chondrocyte implantation: an observational cohort study, Am. J. Sports Med. 38 (6) (2010) 1110–1116.
[7] I. Sekiya, T. Muneta, M. Horie, H. Koga, Arthroscopic transplantation of synovial stem cells improves clinical outcomes in knees with cartilage defects, Clin. Orthop. Relat. Res. 473 (7) (2015) 2316–2326.
[8] Y.S. Kim, Y.J. Choi, Y.G. Koh, Mesenchymal stem cell implantation in knee osteoarthritis: an assessment of the factors influencing clinical outcomes, Am. J. Sports Med. 43 (9) (2015) 2293–2301.
[9] W.S. Toh, C.B. Foldager, M. Pei, J.H. Hui, Advances in mesenchymal stem cell-based strategies for cartilage repair and regeneration, Stem Cell Rev. 10 (5) (2014) 686–696.
[10] S. Meirelles Lda, A.M. Fontes, D.T. Covas, A.I. Caplan, Mechanisms involved in the therapeutic properties of mesenchymal stem cells, Cytokine Growth Factor Rev. 20 (5–6) (2009) 419–427.
[11] H.R. Hofer, R.S. Tuan, Secreted trophic factors of mesenchymal stem cells support neurovascular and musculoskeletal therapies, Stem Cell Res. Ther. 7 (1) (2016) 131.
[12] L. Wu, J.C. Leijten, N. Georgi, J.N. Post, C.A. van Blitterswijk, M. Karperien, Trophic effects of mesenchymal stem cells increase chondrocyte proliferation and matrix formation, Tissue Eng. Part A 17 (9–10) (2011) 1425–1436.
[13] J.H. Lai, G. Kajiyama, R.L. Smith, W. Maloney, F. Yang, Stem cells catalyze cartilage formation by neonatal articular chondrocytes in 3D biomimetic hydrogels, Sci. Rep. 3 (2013) 3553.

[14] R.C. Lai, F. Arslan, M.M. Lee, N.S. Sze, A. Choo, T.S. Chen, M. Salto-Tellez, L. Timmers, C.N. Lee, R.M. El Oakley, G. Pasterkamp, D.P. de Kleijn, S.K. Lim, Exosome secreted by MSC reduces myocardial ischemia/reperfusion injury, Stem Cell Res. 4 (3) (2010) 214–222.

[15] R.C. Lai, R.W. Yeo, S.K. Lim, Mesenchymal stem cell exosomes, Semin. Cell Dev. Biol. 40 (2015) 82–88.

[16] G.W. Hu, Q. Li, X. Niu, B. Hu, J. Liu, S.M. Zhou, S.C. Guo, H.L. Lang, C.Q. Zhang, Y. Wang, Z.F. Deng, Exosomes secreted by human-induced pluripotent stem cell-derived mesenchymal stem cells attenuate limb ischemia by promoting angiogenesis in mice, Stem Cell Res. Ther. 6 (2015) 10.

[17] C. Lee, S.A. Mitsialis, M. Aslam, S.H. Vitali, E. Vergadi, G. Konstantinou, K. Sdrimas, A. Fernandez-Gonzalez, S. Kourembanas, Exosomes mediate the cytoprotective action of mesenchymal stromal cells on hypoxia-induced pulmonary hypertension, Circulation 126 (22) (2012) 2601–2611.

[18] S. Zhang, W.C. Chu, R.C. Lai, S.K. Lim, J.H. Hui, W.S. Toh, Exosomes derived from human embryonic mesenchymal stem cells promote osteochondral regeneration, Osteoarthr. Cartil. 24 (12) (2016) 2135–2140.

[19] R.C. Lai, R.W. Yeo, J. Padmanabhan, A. Choo, D.P. de Kleijn, S.K. Lim, Isolation and characterization of exosome from human embryonic stem cell-derived C-Myc-Immortalized mesenchymal stem cells, Methods Mol. Biol. 1416 (2016) 477–494.

[20] T.S. Chen, F. Arslan, Y. Yin, S.S. Tan, R.C. Lai, A.B. Choo, J. Padmanabhan, C.N. Lee, D.P. de Kleijn, S.K. Lim, Enabling a robust scalable manufacturing process for therapeutic exosomes through oncogenic immortalization of human ESC-derived MSCs, J. Transl. Med. 9 (2011) 47.

[21] W.C. Chu, S. Zhang, T.J. Sng, Y.J. Ong, W.-L. Tan, V.Y. Ang, C.B. Foldager, W.S. Toh, Distribution of pericellular matrix molecules in the temporomandibular joint and their chondroprotective effects against inflammation, Int. J. Oral Sci. 9 (1) (2017) 43–52.

[22] K.A. Jacobson, Introduction to adenosine receptors as therapeutic targets, in: Handbook of Experimental Pharmacology, vol. 193, 2009, pp. 1–24.

[23] W.S. Toh, T.C. Lim, M. Kurisawa, M. Spector, Modulation of mesenchymal stem cell chondrogenesis in a tunable hyaluronic acid hydrogel microenvironment, Biomaterials 33 (15) (2012) 3835–3845.

[24] K.J. Livak, T.D. Schmittgen, Analysis of relative gene expression data using real-time quantitative PCR and the 2(-Delta Delta C(T)) Method, Methods 25 (4) (2001) 402–408.

[25] W.S. Toh, E.H. Lee, M. Richards, T. Cao, In vitro derivation of chondrogenic cells from human embryonic stem cells, Methods Mol. Biol. 584 (2010) 317–331.

[26] W.S. Toh, E.H. Lee, X.-M. Guo, J.K.Y. Chan, C.H. Yeow, A.B. Choo, T. Cao, Cartilage repair using hyaluronan hydrogel-encapsulated human embryonic stem cell-derived chondrogenic cells, Biomaterials 31 (27) (2010) 6968–6980.

[27] W.S. Toh, C.B. Foldager, B.R. Olsen, M. Spector, Basement membrane molecule expression attendant to chondrogenesis by nucleus pulposus cells and mesenchymal stem cells, J. Orthop. Res. 31 (7) (2013) 1136–1143.

[28] N. Fahy, M.L. de Vries-van Melle, J. Lehmann, W. Wei, N. Grotenhuis, E. Farrell, P.M. van der Kraan, J.M. Murphy, Y.M. Bastiaansen-Jenniskens, G.J. van Osch, Human osteoarthritic synovium impacts chondrogenic differentiation of mesenchymal stem cells via macrophage polarisation state, Osteoarthr. Cartil. 22 (8) (2014) 1167–1175.

[29] T. Roszer, Understanding the mysterious M2 macrophage through activation markers and effector mechanisms, Mediat. Inflamm. 2015 (2015) 816460.

[30] S. Wakitani, T. Goto, S.J. Pineda, R.G. Young, J.M. Mansour, A.I. Caplan, V.M. Goldberg, Mesenchymal cell-based repair of large, full-thickness defects of articular cartilage, J. Bone Jt. Surg. Am. 76 (4) (1994) 579–592.

[31] M. Schnabel, S. Marlovits, G. Eckhoff, I. Fichtel, L. Gotzen, V. Vécsei, J. Schlegel, Dedifferentiation-associated changes in morphology and gene expression in primary human articular chondrocytes in cell culture, Osteoarthr. Cartil. 10 (1) (2002) 62–70.

[32] Y. Mishima, M. Lotz, Chemotaxis of human articular chondrocytes and mesenchymal stem cells, J. Orthop. Res. 26 (10) (2008) 1407–1412.

[33] B. Alberts, in: Molecular Biology of the Cell, fourth ed., Garland Science, New York, 2002.

[34] F. Beier, R.F. Loeser, Biology and pathology of Rho GTPase, PI-3 kinase-Akt, and MAP kinase signaling pathways in chondrocytes, J. Cell. Biochem. 110 (3) (2010) 573–580.

[35] D. Ma, X. Kou, J. Jin, T. Xu, M. Wu, L. Deng, L. Fu, Y. Liu, G. Wu, H. Lu, Hydrostatic compress force enhances the viability and decreases the apoptosis of condylar chondrocytes through integrin-FAK-ERK/PI3K pathway, Int. J. Mol. Sci. 17 (11) (2016) 1847.

[36] M. Shakibaei, C. Seifarth, T. John, M. Rahmanzadeh, A. Mobasheri, Igf-I extends the chondrogenic potential of human articular chondrocytes in vitro: molecular association between Sox9 and Erk1/2, Biochem. Pharmacol. 72 (11) (2006) 1382–1395.

[37] R.C. Lai, S.S. Tan, B.J. Teh, S.K. Sze, F. Arslan, D.P. de Kleijn, A. Choo, S.K. Lim, Proteolytic potential of the MSC exosome proteome: implications for an exosome-mediated delivery of therapeutic proteasome, Int. J. Proteomics 2012 (2012) 14.

[38] R. Lai, R. Yeo, S. Tan, B. Zhang, Y. Yin, N. Sze, A. Choo, S. Lim, Mesenchymal stem cell exosomes: the future MSC-based therapy?, in: L.G. Chase, M.C. Vemuri (Eds.), Mesenchymal Stem Cell Therapy, Humana Press, 2013, pp. 39–61.

[39] C.T. Lim, X. Ren, M.H. Afizah, S. Tarigan-Panjaitan, Z. Yang, Y. Wu, K.S. Chian, A.G. Mikos, J.H. Hui, Repair of osteochondral defects with rehydrated freeze-dried oligo[poly(ethylene glycol) fumarate] hydrogels seeded with bone marrow mesenchymal stem cells in a porcine model, Tissue Eng. Part A 19 (15–16) (2013) 1852–1861.

[40] W.S. Toh, R.C. Lai, J.H. Hui, S.K. Lim, MSC exosome as a cell-free MSC therapy for cartilage regeneration: implications for osteoarthritis treatment, Semin. Cell Dev. Biol. 67 (2017) 56–64.

[41] R.C. Lai, S.S. Tan, R.W.Y. Yeo, A.B.H. Choo, A.T. Reiner, Y. Su, Y. Shen, Z. Fu, L. Alexander, S.K. Sze, S.K. Lim, MSC secretes at least 3 EV types each with a unique permutation of membrane lipid, protein and RNA, J. Extracell. Vesicles 5 (1) (2016).

[42] B. Zhang, M. Wang, A. Gong, X. Zhang, X. Wu, Y. Zhu, H. Shi, L. Wu, W. Zhu, H. Qian, W. Xu, HucMSC-exosome mediated-Wnt4 signaling is required for cutaneous wound healing, Stem Cells 33 (7) (2015) 2158–2168.

[43] J. Zhang, X. Liu, H. Li, C. Chen, B. Hu, X. Niu, Q. Li, B. Zhao, Z. Xie, Y. Wang, Exosomes/tricalcium phosphate combination scaffolds can enhance bone regeneration by activating the PI3K/Akt signaling pathway, Stem Cell Res. Ther. 7 (1) (2016) 136.

[44] F. Arslan, R.C. Lai, M.B. Smeets, L. Akeroyd, A. Choo, E.N. Aguor, L. Timmers, H.V. van Rijen, P.A. Doevendans, G. Pasterkamp, S.K. Lim, D.P. de Kleijn, Mesenchymal stem cell-derived exosomes increase ATP levels, decrease oxidative stress and activate PI3K/Akt pathway to enhance myocardial viability and prevent adverse remodeling after myocardial ischemia/reperfusion injury, Stem Cell Res. 10 (3) (2013) 301–312.

[45] H.Y. Qureshi, R. Ahmad, J. Sylvester, M. Zafarullah, Requirement of phosphatidylinositol 3-kinase/Akt signaling pathway for regulation of tissue inhibitor of metalloproteinases-3 gene expression by TGF-beta in human chondrocytes, Cell. Signal. 19 (8) (2007) 1643–1651.

[46] H.Y. Qureshi, J. Sylvester, M. El Mabrouk, M. Zafarullah, TGF-beta-induced expression of tissue inhibitor of metalloproteinases-3 gene in chondrocytes is mediated by extracellular signal-regulated kinase pathway and Sp1 transcription factor, J. Cell Physiol. 203 (2) (2005) 345–352.

[47] B. Gharibi, M.S. Ghuman, F.J. Hughes, Akt- and Erk-mediated regulation of proliferation and differentiation during PDGFRbeta-induced MSC self-renewal, J. Cell Mol. Med. 16 (11) (2012) 2789–2801.

[48] K. Nakamura, T. Shirai, S. Morishita, S. Uchida, K. Saeki-Miura, F. Makishima, p38 mitogen-activated protein kinase functionally contributes to chondrogenesis induced by growth/differentiation factor-5 in ATDC5 cells, Exp. Cell Res. 250 (2) (1999) 351–363.

[49] S.C. Tao, T. Yuan, Y.L. Zhang, W.J. Yin, S.C. Guo, C.Q. Zhang, Exosomes derived from miR-140-5p-overexpressing human synovial mesenchymal stem cells enhance cartilage tissue regeneration and prevent osteoarthritis of the knee in a rat model, Theranostics 7 (1) (2017) 180–195.

[50] J. Lieberthal, N. Sambamurthy, C.R. Scanzello, Inflammation in joint injury and post-traumatic osteoarthritis, Osteoarthr. Cartil. 23 (11) (2015) 1825–1834.

[51] B.J. Heard, K.I. Barton, M. Chung, Y. Achari, N.G. Shrive, C.B. Frank, D.A. Hart, Single intra-articular dexamethasone injection immediately post-surgery in a rabbit model mitigates early inflammatory responses and post-traumatic osteoarthritis-like alterations, J. Orthop. Res. 33 (12) (2015) 1826–1834.

[52] J. Ding, B. Chen, T. Lv, X. Liu, X. Fu, Q. Wang, L. Yan, N. Kang, Y. Cao, R. Xiao, Bone marrow mesenchymal stem cell-based engineered cartilage ameliorates polyglycolic acid/polylactic acid scaffold-induced inflammation through M2 polarization of macrophages in a pig model, Stem Cells Transl. Med. 5 (8) (2016) 1079–1089.

[53] L. Utomo, Y.M. Bastiaansen-Jenniskens, J.A. Verhaar, G.J. van Osch, Cartilage inflammation and degeneration is enhanced by pro-inflammatory (M1) macrophages in vitro, but not inhibited directly by anti-inflammatory (M2) macrophages, Osteoarthr. Cartil. 24 (12) (2016) 2162–2170.

[54] Y. Zhang, T. Pizzute, M. Pei, Anti-inflammatory strategies in cartilage repair, Tissue Eng. Part B, Rev. 20 (6) (2014) 655–668.

[55] B. Zhang, Y. Yin, R.C. Lai, S.S. Tan, A.B. Choo, S.K. Lim, Mesenchymal stem cells secrete immunologically active exosomes, Stem Cells Dev. 23 (11) (2014) 1233–1244.

[56] A.T. Reiner, K.W. Witwer, B.W.M. van Balkom, J. de Beer, C. Brodie, R.L. Corteling, S. Gabrielsson, M. Gimona, A.G. Ibrahim, D. de Kleijn, C.P. Lai, J. Lötvall, H.A. del Portillo, I.G. Reischl, M. Riazifar, C. Salomon, H. Tahara, W.S. Toh, M.H.M. Wauben, V.K. Yang, Y. Yang, R.W.Y. Yeo, H. Yin, B. Giebel, E. Rohde, S.K. Lim, Concise review: developing best-practice models for the therapeutic use of extracellular vesicles, Stem Cells Transl. Med. 6 (8) (2017) 1730–1739.